Helicity Thinkshop 3
19-23 November 2017, Tokyo, Japan

Characteristics of Magnetic Helicity Flux in the Solar Active Region Photosphere

Sung-Hong Park[1], KD Leka[1,2], Kanya Kusano[1]

[1] Institute for Space-Earth Environmental Research, Nagoya University, Japan
[2] NorthWest Research Associates, Boulder, CO, USA

Many thanks to the ***EU FLARECAST*** team

名古屋大学 NAGOYA UNIVERSITY

ISEE Nagoya university Institute for Space-Earth Environmental Research

NWRA Since 1984

1. Hemispheric Helicity Sign "Preference"

(Image credit: A. Pevtsov)

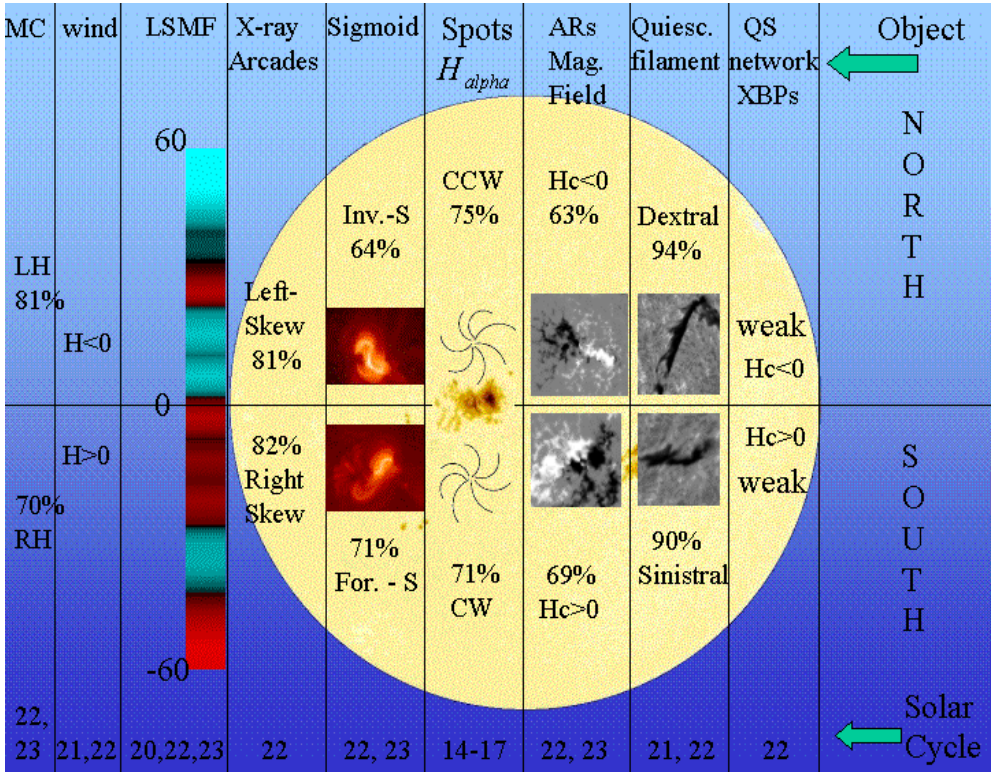

This may be attributed to:

- Differential rotation (Démoulin et al. 2002)
- Coriolis force (Holder et al. 2004)
- Helical convective turbulence Σ-effect (Longcope et al. 1999)
- Subsurface dynamo (Gilman & Charbonneau 1999)

Q1: What about Solar Cycle 24?

- Weakest solar cycle in more than a century
- SDO/HMI full-disk vector magnetograms @ 12-min cadence since 2010

2. Helicity Flux in Solar Active Regions

Berger &Field (1984)

$$\frac{\mathrm{d}H}{\mathrm{d}t} = 2\int_S \left(\boldsymbol{A}_p \cdot \boldsymbol{B}_h\right) v_n \,\mathrm{d}S - 2\int_S \left(\boldsymbol{A}_p \cdot \boldsymbol{v}_h\right) B_n \,\mathrm{d}S$$

<TERMS>

- dH/dt [Mx^2/s]
  - Relative magnetic helicity flux across the active region photospheric surface S
- B_n & $\boldsymbol{B}_h$ [G]
  - Photospheric vector magnetic field with n denoting the normal component to S and t the tangential vector
- A_p [G•m]
  - Vector potential of the corresponding current-free, potential field
- v_n & $\boldsymbol{v}_h$ [m/s]
  - Photospheric plasma velocity perpendicular to the magnetic field

2.1. SDO/HMI Vector Magnetic Field (*B*)

Spaceweather HMI Active Region Patch (SHARP)

- ***HARP***: Automatically-identified active region patches of line-of-sight and vector magnetic field, continuum intensity, Doppler velocity
- ***Cadence***: 720-sec (12-min)
- ***CEA***: Lambert Cylindrical Equal-Area projection and decomposed into B_r, B_p, B_t
- ***NRT***: Near real time / preliminary calibrations (Hoeksema et al. 2014) & faster disambiguation code (Bobra et al. 2014)

2.2. Current-free Vector Potential (A_p)

Fast Fourier Transform Method (Chae 2001)

$$A_{p,x} = \mathrm{FT}^{-1}\left(\frac{\mathrm{i}k_y}{k_x^2 + k_y^2}\,\mathrm{FT}(B_z)\right)$$

$$A_{p,y} = \mathrm{FT}^{-1}\left(-\frac{\mathrm{i}k_x}{k_x^2 + k_y^2}\,\mathrm{FT}(B_z)\right)$$

$$\mathrm{FT}(B_z) = \Sigma_{x,y} B_z(\mathrm{x,y}) \exp(-\mathrm{i}k_x x - \mathrm{i}k_y y)$$

2.3. Plasma Flow Velocity Field (*v*)

DAVE4VM (Schuck 2006)

- **D**ifferential **A**ffine **V**elocity **E**stimator for **V**ector **M**agnetograms
- Plasma flow estimation from vector magnetograms solving the MHD induction equation of an ideal conductive fluid

Normal component of the induction equation

$$\partial_t B_z + \boldsymbol{\nabla}_h \cdot \left(B_z\, \boldsymbol{v}_h - v_z\, \boldsymbol{B}_h\right) = 0$$

Iterative least-square inversion with an apodizing window *w* having the affine velocity profile

$$\mathcal{C}_{\mathrm{SSD}} = \int dt dx^2 \boxed{w\left(\boldsymbol{x}-\boldsymbol{\chi}, t-\tau\right)} \{\partial_t B_z\left(\boldsymbol{x}, t\right) + \boldsymbol{\nabla}_h \cdot \left[B_z\left(\boldsymbol{x}, t\right)\, \boldsymbol{v}_h\left(\boldsymbol{P}, \boldsymbol{x}-\boldsymbol{\chi}\right)\,, -v_z\left(\boldsymbol{P}, \boldsymbol{x}-\boldsymbol{\chi}\right)\, \boldsymbol{B}_h\left(\boldsymbol{x}, t\right)\right]\}^2$$

Affine velocity profile

$$\boldsymbol{v}\left(\boldsymbol{P}; \boldsymbol{x}\right) = \begin{pmatrix} \widehat{u}_0 \\ \widehat{v}_0 \\ \widehat{w}_0 \end{pmatrix} + \begin{pmatrix} \widehat{u}_x & \widehat{u}_y \\ \widehat{v}_x & \widehat{v}_y \\ \widehat{w}_x & \widehat{w}_y \end{pmatrix} \begin{pmatrix} x \\ y \end{pmatrix} \qquad \text{where} \qquad \widehat{u}_x = \partial_x\left(\widehat{\boldsymbol{x}} \cdot \boldsymbol{v}\right)$$

Tests on Apodizing Window Size for DAVE4VM

- Data: SHARP CEA NRT vector magnetic field data @ 12-min cadence
- Window size: 15 pixels

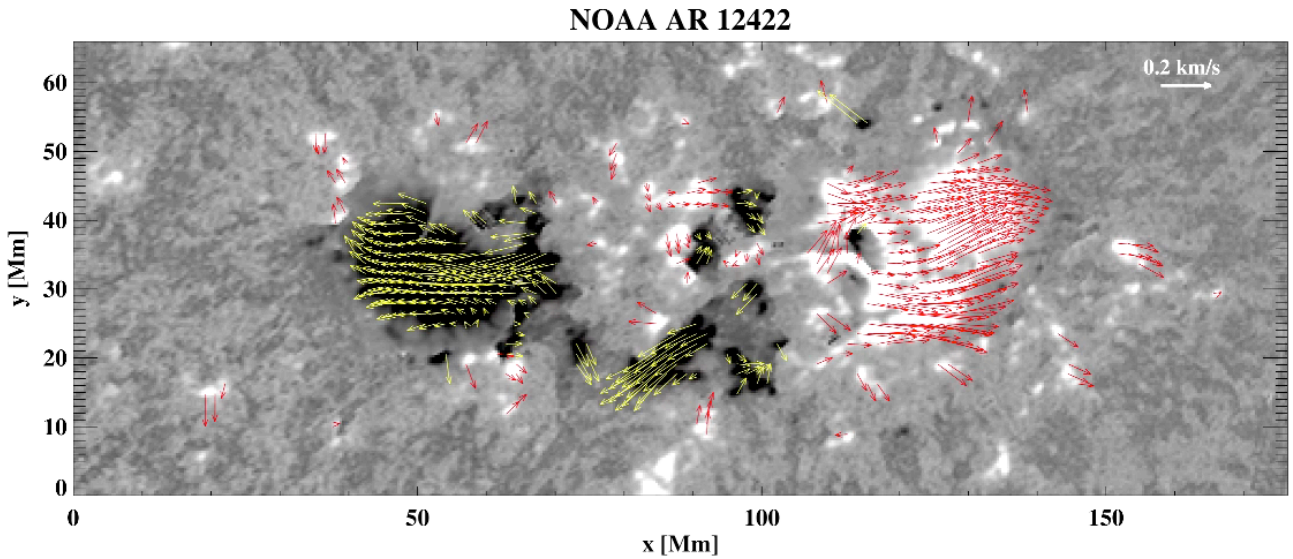

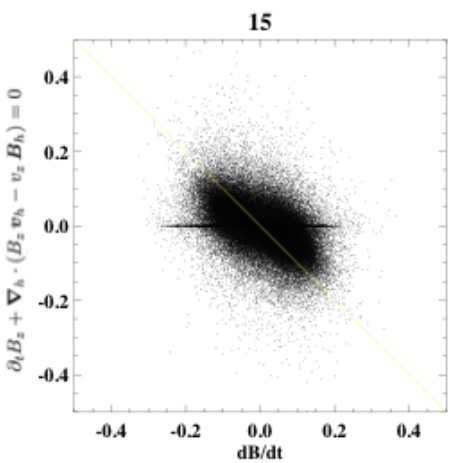

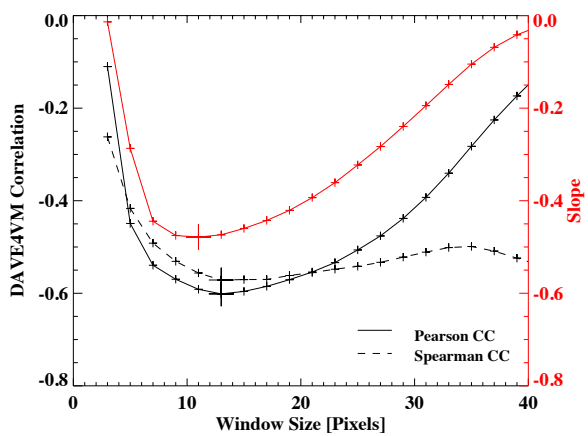

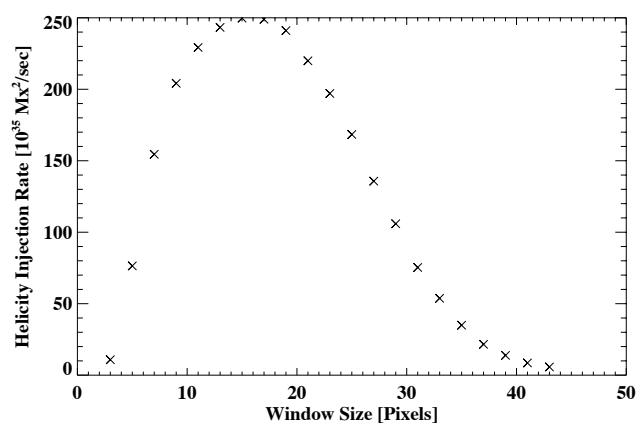

2.4. Active Region Dataset

- In total of 3,239 NOAA numbered regions within ±50 degrees from the central meridian
  : 2,922 ARs with sunspots (882 different NOAA numbered regions)
  : 317 spotless Ha plage regions

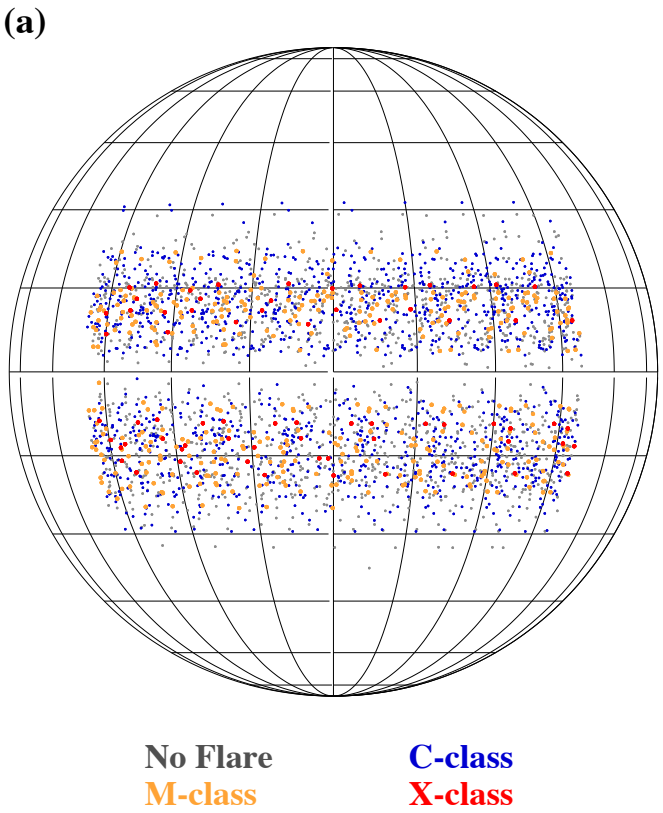

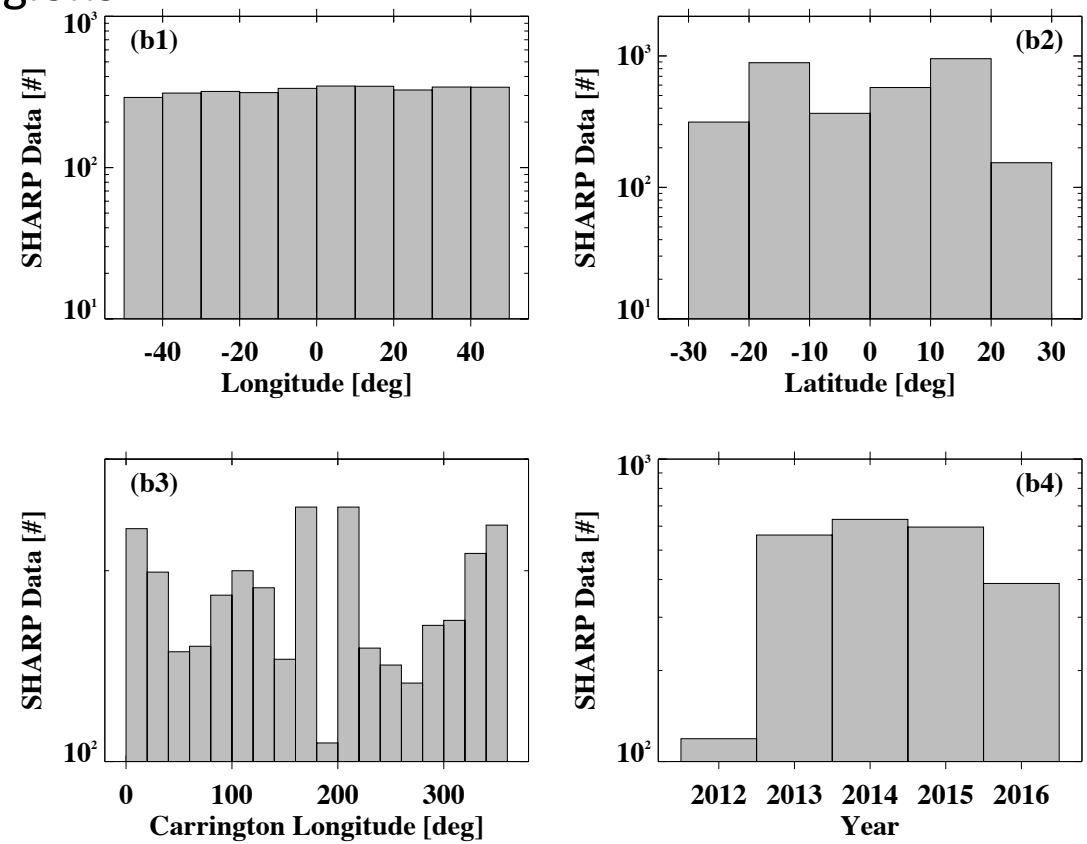

3. Results

Frequency Distribution of Helicity Flux Density

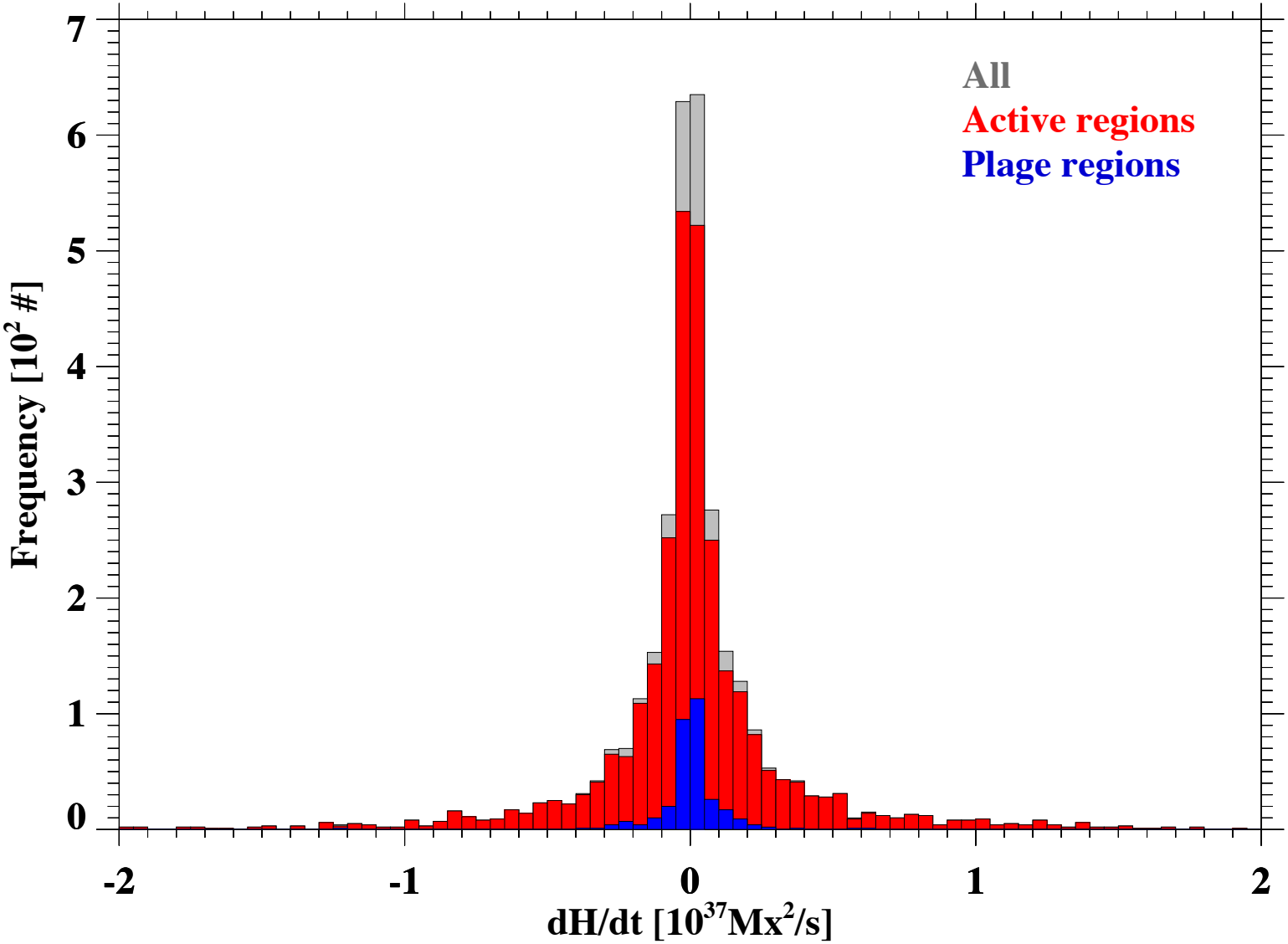

Sunspot NOAA numbered ARs ONLY!

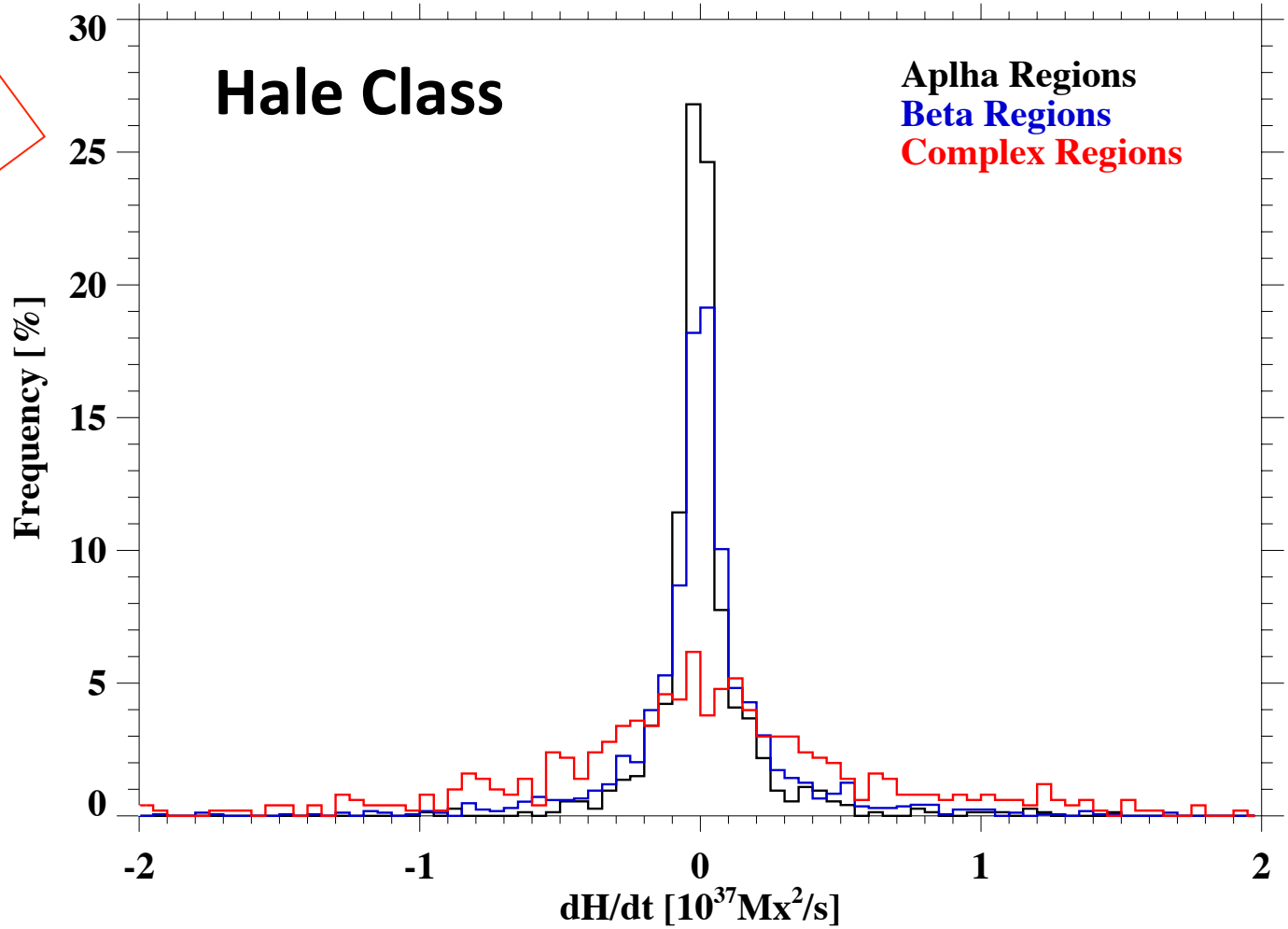

	Northern			Southern		
	Mean	Std Dev	Negative (%)	Mean	Std Dev	Positive (%)
Alpha	-0.01	0.16	59	0.05	0.23	56
Beta	-0.04	0.28	54	0.07	0.30	60
Complex	-0.22	0.57	65	0.21	0.58	62

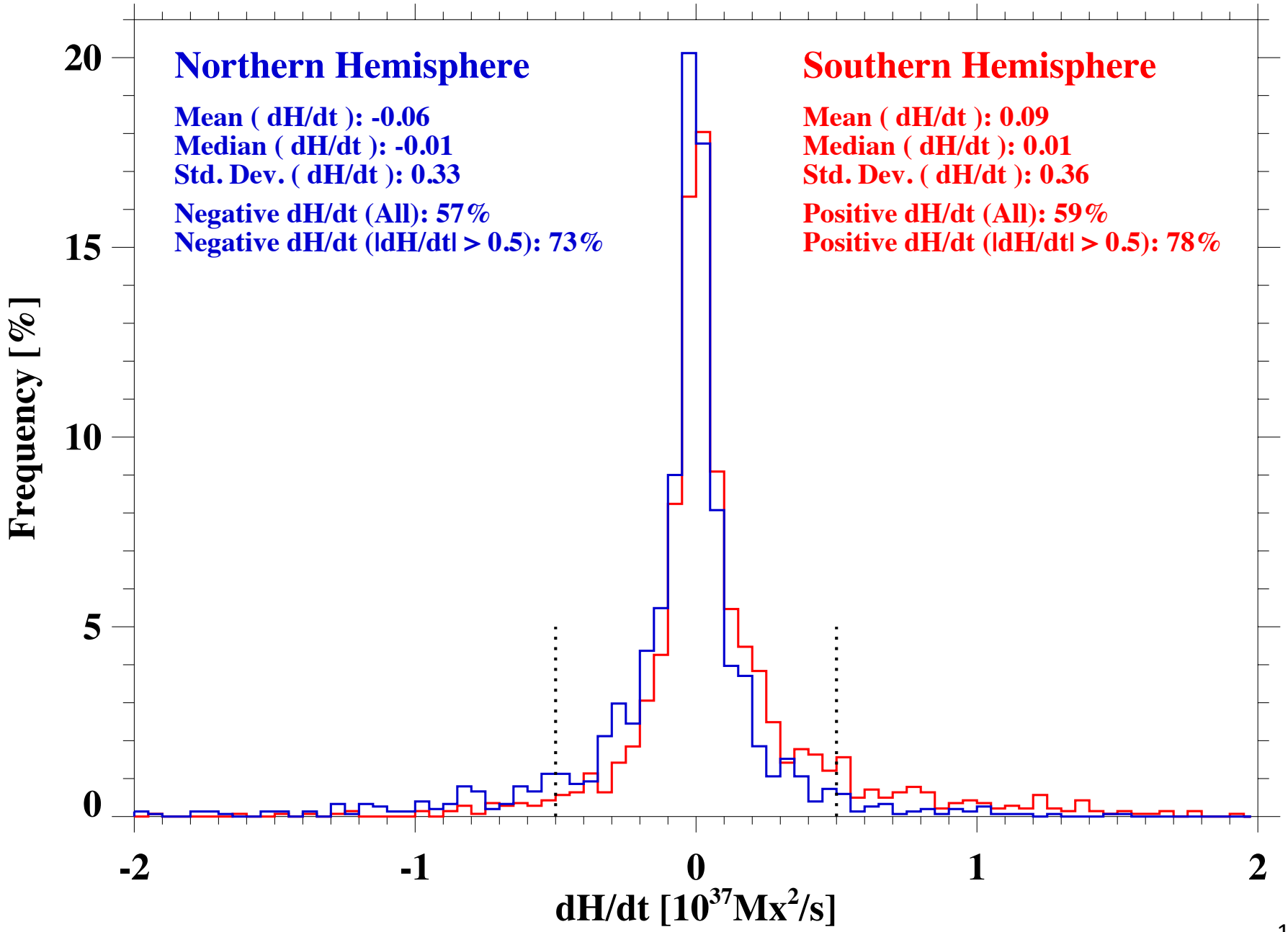
Northern Hemisphere
Mean (dH/dt): -0.06
Median (dH/dt): -0.01
Std. Dev. (dH/dt): 0.33
Negative dH/dt (All): 57%
Negative dH/dt (|dH/dt| > 0.5): 73%
Southern Hemisphere
Mean (dH/dt): 0.09
Median (dH/dt): 0.01
Std. Dev. (dH/dt): 0.36
Positive dH/dt (All): 59%
Positive dH/dt (|dH/dt| > 0.5): 78%
Frequency [%]
20
15
10
5
0
-2
-1
0
1
2
dH/dt [10^37 Mx^2/s]

2D Histogram of dH/dt and Latitude

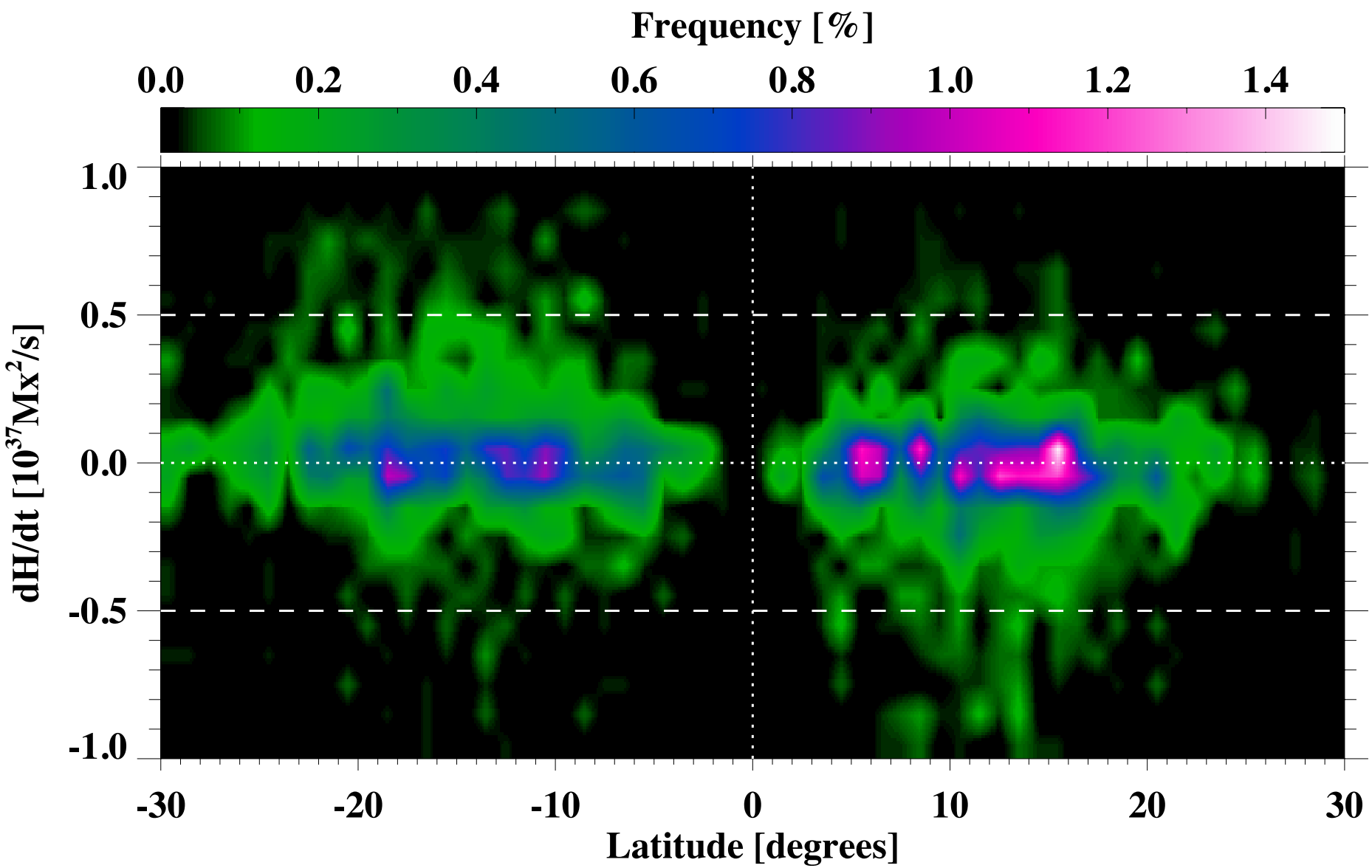

4. Conclusions

- **The hemispheric helicity sign preference is there in Solar Cycle 24**.
  - Weak tendency of negative dH/dt in the northern hemisphere (57%) and positive dH/dt in the southern hemisphere (59%).
  - This tendency becomes much stronger (73% in North, 78% in South) in ARs with large dH/dt.